The Star Formation Newsletter

A community newsletter on Star and Planet Formation research

No. 344 — 22 August 2021
Editor: João Alves www.starformation.news

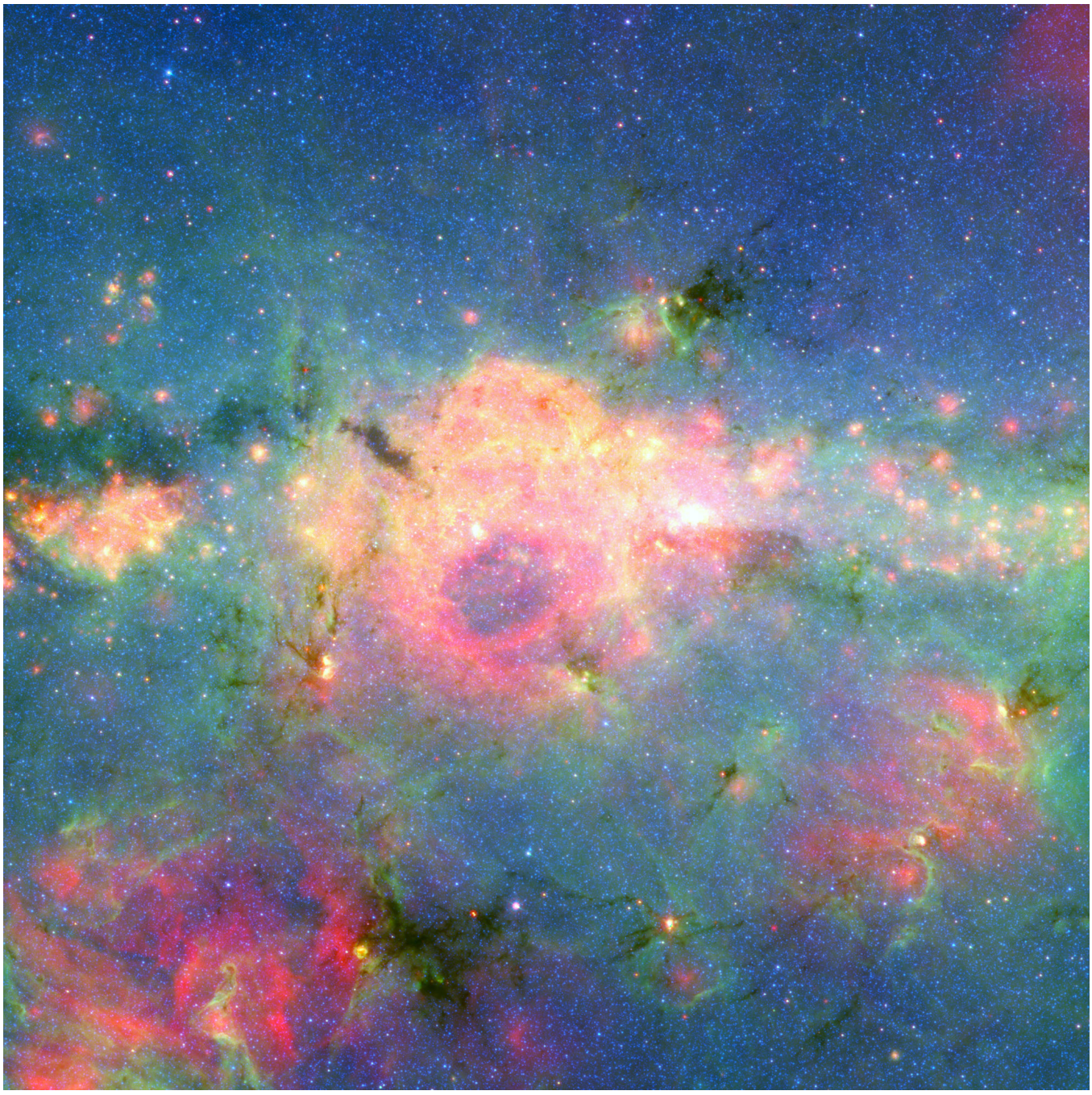

Links to sections

Interviews	Reviews	Perspective	Favorite objects	Archive
Meetings	Jobs	New PhDs	Announcements	Books

Cover image caption

Mid-Infrared color composite of the Galactic Center. Once Terra Incognita, the Galactic Center is becoming a major star formation target in recent years. For scale, the image's width, about 250 pc at a distance of 8.3 kpc, is about the size of the entire Orion star formation region. Over the last few years, major work has focused on, e.g., Sgr B2, the Brick, the Arches and Quintuplet clusters, and the enigmatic Galactic Center cluster. Credit: NASA, JPL-Caltech.

Note from the Editor

The Star Formation Newsletter is now on the web at **www.starformation.news**. This PDF file contains the monthly Abstracts and links to the different Newsletter sections. Red text in this PDF is a url link. Submitting an abstract to the SFN is as simple as entering the arXiv ID (e.g., 2006.10139) in a web form on the SFN web site. **Do not remove the LaTeX formatting when submitting to the arXiv**. If you do, your abstract will not look great either at the arXiv (which uses MathJax to convert LaTeX math symbols to the web) or the SFN.

Abstracts

1. A Circumplanetary Disk Around PDS70c

Myriam Benisty, Jaehan Bae, Stefano Facchini, Miriam Keppler, Richard Teague, Andrea Isella, Nicolas T. Kurtovic, Laura M. Perez, Anibal Sierra, Sean M. Andrews, John Carpenter, Ian Czekala, Carsten Dominik, Thomas Henning, Francois Menard, Paola Pinilla, Alice Zurlo

PDS70 is a unique system in which two protoplanets, PDS70b and c, have been discovered within the dust-depleted cavity of their disk, at ∼22 and 34au respectively, by direct imaging at infrared wavelengths. Subsequent detection of the planets in the Hα line indicates that they are still accreting material through circumplanetary disks. In this Letter, we present new Atacama Large Millimeter/submillimeter Array (ALMA) observations of the dust continuum emission at 855μm at high angular resolution (∼20mas, 2.3au) that aim to resolve the circumplanetary disks and constrain their dust masses. Our observations confirm the presence of a compact source of emission co-located with PDS70c, spatially separated from the circumstellar disk and less extended than ∼1.2au in radius, a value close to the expected truncation radius of the cicumplanetary disk at a third of the Hill radius. The emission around PDS70c has a peak intensity of ∼86±16 μJy beam^{-1} which corresponds to a dust mass of ∼0.031M$_\oplus$ or ∼0.007M$_\oplus$, assuming that it is only constituted of 1 μm or 1 mm sized grains, respectively. We also detect extended, low surface brightness continuum emission within the cavity near PDS70b. We observe an optically thin inner disk within 18au of the star with an emission that could result from small micron-sized grains transported from the outer disk through the orbits of b and c. In addition, we find that the outer disk resolves into a narrow and bright ring with a faint inner shoulder.

2. The Substructures in Disks undergoing Vertical Shear Instability: II. Observational Predictions for the Dust Continuum

Diana Blanco, Luca Ricci, Mario Flock, Neal Turner

High-angular resolution observations at sub-millimeter/millimeter wavelengths of disks surrounding young stars have shown that their morphology is made of azimuthally-symmetric or point-symmetric substructures, in some cases with spiral arms, localized spur- or crescent-shaped features. The majority of theoretical studies with the aim of interpreting the observational results have focused on disk models with planets, under the assumption that the disk substructures are due to the disk-planet interaction. However, so far only in very few cases exoplanets have been detected in these systems. Furthermore, some substructures are expected to appear *before* planets form, as they are necessary to drive the concentration of small solids which can lead to the formation of planetesimals. In this work we present observational predictions from high-resolution 3D radiative hydrodynamical

models which follow the evolution of gas and solids in a protoplanetary disk. We focus on substructures in the distribution of millimeter-sized and smaller solid particles produced by the vertical shear instability. We show that their characteristics are compatible with some of the shallow gaps detected in recent observations at sub-mm/mm wavelengths, and present predictions for future observations with better sensitivity and angular resolution with ALMA and a Next Generation Very Large Array.

3. Hourglass Magnetic Field from a Survey of Current Density Profiles

Gianfranco Bino, Shantanu Basu, Mahmoud Sharkawi, Indrani Das

Modelling the magnetic field in prestellar cores can serve as a useful tool for studying the initial conditions of star formation. The analytic hourglass model of Ewertowski and Basu (2013) provides a means to fit observed polarimetry measurements and extract useful information. The original model does not specify any radial distribution of the electric current density. Here, we perform a survey of possible centrally-peaked radial distributions of the current density, and numerically derive the full hourglass patterns. Since the vertical distribution is also specified in the original model, we can study the effect of different ratios of vertical to radial scale length on the overall hourglass pattern. Different values of this ratio may correspond to different formation scenarios for prestellar cores. We demonstrate the flexibility of our model and how it can be applied to a variety of magnetic field patterns.

4. The STAR-MELT Python package for emission line analysis of YSOs

Justyn Campbell-White, Aurora Sicilia-Aguilar, Carlo F. Manara, Soko Matsumura, Min Fang, Antonio Frasca, Veronica Roccatagliata

We introduce the STAR-MELT Python package that we developed to facilitate the analysis of time-resolved emission line spectroscopy of young stellar objects. STAR-MELT automatically extracts, identifies and fits emission lines. We summarise our analysis methods that utilises the time domain of high-resolution stellar spectra to investigate variability in the line profiles and corresponding emitting regions. This allows us to probe the innermost disc and accretion structures of YSOs. Local temperatures and densities can be determined using Boltzmann statistics, the Saha equation, and the Sobolev large velocity gradient approximation. STAR-MELT allows for new results to be obtained from archival data, as well as facilitating timely analysis of new data as it is obtained. We present the results of applying STAR-MELT to three YSOs, using spectra from UVES, XSHOOTER, FEROS, HARPS, and ESPaDOnS. We demonstrate what can be achieved for data with disparate time sampling, for stars with different inclinations and variability types. For EX Lupi, we confirm the presence of a localised and stable stellar-surface hot spot associated with the footprint of the accretion column. For GQ Lupi A, we find that the maximum infall rate from an accretion column is correlated with lines produced in the lowest temperatures. For CVSO109 we investigate the rapid temporal variability of a redshifted emission wing, indicative of rotating and infalling material in the inner disc. Our results show that STAR-MELT is a useful tool for such analysis, as well as other applications for emission lines.

5. Core mass function of a single giant molecular cloud complex with 10^4 cores

Yue Cao, Keping Qiu, Qizhou Zhang, Yuwei Wang, Yuanming Xiao

Similarity in shape between the initial mass function (IMF) and the core mass functions (CMFs) in star-forming regions prompts the idea that the IMF originates from the CMF through a self-similar core-to-star mass mapping process. To accurately determine the shape of the CMF, we create a sample of 8,431 cores with the dust continuum maps of the Cygnus X giant molecular cloud complex, and design a procedure for deriving the CMF considering the mass uncertainty, binning uncertainty, sample incompleteness, and the statistical errors. The resultant CMF coincides well with the IMF for core masses from a few $M_\odot$ to the highest masses of 1300 $M_\odot$ with a power-law of $\mathrm{d}N/\mathrm{d}M \propto M^{-2.30\pm0.04}$, but does not present an obvious flattened turnover in the low-mass range as the IMF does. More detailed inspection reveals that the slope of the CMF steepens with increasing mass. Given the numerous high-mass star-forming activities of Cygnus X, this is in stark contrast with the existing top-heavy CMFs found in high-mass star-forming clumps. We also find that the similarity between the IMF and the mass function of cloud structures is not unique at core scales, but can be seen for cloud structures of up to several pc scales. Finally, our SMA observations toward a subset of the cores do not present evidence for the self-similar mapping. The latter two results indicate that the shape of the IMF may not be directly inherited from the CMF.

6. The GUAPOS project II. A comprehensive study of peptide-like bond molecules

L. Colzi, V. M. Rivilla, M. T. Beltrán, I. Jiménez-Serra, C. Mininni, M. Melosso, R. Cesaroni, F. Fontani, A. Lorenzani, A. Sánchez-Monge, S. Viti, P. Schilke, L. Testi, E. R. Alonso, L. Kolesniková

Peptide-like bond molecules, which can take part to the formation of proteins in a primitive Earth environment, have been detected up to now only towards a few sources. We present a study of HNCO, $HC(O)NH_2$, CH_3NCO, $CH_3C(O)NH_2$, CH_3NHCHO, CH_3CH_2NCO, $NH_2C(O)NH_2$, $NH_2C(O)CN$, and $HOCH_2C(O)NH_2$ towards the hot core G31.41+0.31. We have used the spectrum obtained from the ALMA 3mm spectral survey GUAPOS, with an angular resolution of 1.2"×1.2" (∼4500 au), to derive column densities of all the molecular species, together with other 0.2"×0.2" (∼750 au) ALMA observations to study the morphology of HNCO, $HC(O)NH_2$ and $CH_3C(O)NH_2$. We have detected HNCO, $HC(O)NH_2$, CH_3NCO, $CH_3C(O)NH_2$, and CH_3NHCHO, for the first time all together outside the Galactic center. We have obtained molecular fractional abundances with respect to H_2 from 10^{-7} down to a few 10^{-9} and with respect to CH_3OH from 10^{-3} to $\sim 4\times10^{-2}$. From the comparison with other sources, we find that regions in an earlier stage of evolution, such as pre-stellar cores, show abundances at least two orders of magnitude lower than those in hot cores, hot corinos or shocked regions. Moreover, molecular abundance ratios towards different sources are found to be consistent between them within ∼1 order of magnitude, regardless of the physical properties (e.g. different masses and luminosities), or the source position throughout the Galaxy. New correlations between pairs of molecular abundances have also been found. These results suggest that all these species are formed on grain surfaces in early evolutionary stages of molecular clouds, and that they are subsequently released back to the gas-phase through thermal desorption or shock-triggered desorption.

7. A survey for variable young stars with small telescopes: IV – Rotation Periods of YSOs in IC5070

Dirk Froebrich, Efthymia Derezea, Aleks Scholz, Jochen Eislöffel, Siegfried Vanaverbeke, Alfred Kume, Carys Herbert, Justyn Campbell-White, Niall Miller, Bringfried Stecklum, Sally V. Makin, Thomas Urtly, Francisco C. Soldán Alfaro, Erik Schwendeman, Geoffrey Stone, Mark Phillips, George Fleming, Rafael Gonzalez Farfán, Tonny Vanmunster, Michael A. Heald, Esteban Fernández Mañanes, Tim Nelson, Heinz-Bernd Eggenstein, Franky Dubois, Ludwig Logie, Steve Rau, Klaas Wiersema, Nick Quinn, Diego Rodriguez, Rafael Castillo García, Thomas Killestein, Tony Vale, Domenico Licchelli, Marc Deldem, Georg Piehler, Dawid Moździerski, Krzysztof Kotysz, Katarzyna Kowalska, Przemysław Mikołajczyk, Stephen R. L. Futcher, Timothy P. Long, Mario Morales Aimar, Barry Merrikin, Stephen Johnstone, Pavol A. Dubovský, Igor Kudzej, Roger Pickard, Samuel J. Billington, Lord Dover, Tarik Zegmott, Jack J. Evitts, Alejandra Traspas Munia, Mark C. Price

Studying rotational variability of young stars is enabling us to investigate a multitude of properties of young star-disk systems. We utilise high cadence, multi-wavelength optical time series data from the Hunting Outbursting Young Stars citizen science project to identify periodic variables in the Pelican Nebula (IC5070). A double blind study using nine different period-finding algorithms was conducted and a sample of 59 periodic variables was identified. We find that a combination of four period finding algorithms can achieve a completeness of 85% and a contamination of 30% in identifying periods in inhomogeneous data sets. The best performing methods are periodograms that rely on fitting a sine curve. Utilising GaiaEDR3 data, we have identified an unbiased sample of 40 periodic YSOs, without using any colour or magnitude selections. With a 98.9% probability we can exclude a homogeneous YSO period distribution. Instead we find a bi-modal distribution with peaks at three and eight days. The sample has a disk fraction of 50%, and its statistical properties are in agreement with other similarly aged YSOs populations. In particular, we confirm that the presence of the disk is linked to predominantly slow rotation and find a probability of 4.8×10^{-3} that the observed relation between period and presence of a disk has occurred by chance. In our sample of periodic variables, we also find pulsating giants, an eclipsing binary, and potential YSOs in the foreground of IC5070.

8. CRAFT (Cosmic Ray Acceleration From Turbulence) in Molecular Clouds

Brandt A. L. Gaches, Stefanie Walch, Alex Lazarian

Low-energy cosmic rays, in particular protons with energies below 1 GeV, are significant drivers of the thermochemistry of molecular clouds. However, these cosmic rays are also greatly impacted by energy losses and magnetic field transport effects in molecular gas. Explaining cosmic ray ionization rates of 10^{-16} s^{-1} or greater in dense gas requires either a high external cosmic ray flux, or local sources of MeV-GeV cosmic ray protons. We present a new local source of low-energy cosmic rays in molecular clouds: first order Fermi-acceleration of protons in regions undergoing turbulent reconnection in molecular clouds. We show from energetic-based arguments there is sufficient energy within the magneto-hydrodynamic turbulent cascade to produce ionization rates compatible with inferred ionization rates in molecular clouds. As turbulent reconnection is a volume-filling process, the proposed mechanism can produce a near-homogeneous distribution of low-energy cosmic rays within molecular clouds.

9. Touching the Stars: Using High-Resolution 3D Printing to Visualize Stellar Nurseries

Nia Imara, John C. Forbes, James C. Weaver

Owing to their intricate variable density architecture, and as a principal site of star formation, molecular clouds represent one of the most functionally significant, yet least understood features of our universe. To unravel the intrinsic structural complexity of molecular clouds, here we leverage the power of high-resolution bitmap-based 3D printing, which provides the opportunity to visualize astrophysical structures in a way that uniquely taps into the human brain's ability to recognize patterns suppressed in 2D representations. Using a new suite of nine simulations, each representing different physical extremes in the turbulent interstellar medium, as our source data, our workflow permits the unambiguous visualization of features in the 3D-printed models, such as quasi-planar structures, that are frequently obscured in traditional renderings and animations. Our bitmap-based 3D printing approach thus faithfully reproduces the subtle density gradient distribution within molecular clouds in a tangible, intuitive, and visually stunning manner. While laying the groundwork for the intuitive analysis of other structurally complex astronomical data sets, our 3D-printed models also serve as valuable tools in educational and public outreach endeavors.

10. Dark cloud-type chemistry in PDRs with moderate UV field

Maria S. Kirsanova, Anna F. Punanova, Dmitry A. Semenov, Anton I. Vasyunin

We present a study of emission lines of small hydrocarbons C_2H and c-C_3H_2, and COMs precursors H_2CO and CH_3OH in order to better understand the possible chemical link between the molecular abundances and UV radiation field in photodissociation regions (PDRs). We study two PDRs around extended and compact HII regions with $G \leq 50$ Habings in the S235 star-forming complex. We find the highest abundances of both hydrocarbons on the edges of molecular clumps, while c-C_3H_2 is also abundant in the low-density expanding PDR around compact HII region S235 A. We see the highest methanol column density towards the positions with the UV field $G \approx 20 - 30$ Habings and explain them by reactive desorption from the dust grains. The N_{C_2H}/N_{CH_3OH} ratio is lower by a factor of few or the order of magnitude in comparison with the Horsehead and Orion Bar PDRs. The ratio is similar to the value observed in hot corinos in the Perseus cloud. We conclude that ion-molecular and grain surface chemical routes rule the molecular abundances in the PDRs, and the PDRs inherit molecular abundances from the previous dark stage of molecular cloud evolution in spite of massive stars already emitting in optics.

11. The first interferometric survey in the K-band of massive YSOs. On the hot dust, ionised gas, and binarity at au scales

E. Koumpia, W. -J. de Wit, R. D. Oudmaijer, A. J. Frost, S. Lumsden, A. Caratti o Garatti, S. P. Goodwin, B. Stecklum, I. Mendigutıa, J. D. Ilee, M. Vioque

Circumstellar discs are essential for high mass star formation, while multiplicity, in particular binarity, appears to be an inevitable outcome since the vast majority of massive stars ($>$ 8 Msun) are found in binaries (up to 100%). We constrain the sizes of the dust and ionised gas (Brgamma) emission of the innermost regions towards a sample of six MYSOs, and provide high-mass binary statistics of young stars at 2-300 au scales using VLTI (GRAVITY, AMBER) observations. We determine the inner radius of the dust emission and place MYSOs with K-band measurements in a size-luminosity diagram for the first time, and compare our findings to T Tauris and Herbig AeBes. We also compare the observed K-band sizes to the sublimation radius predicted by three different disc scenarios. Lastly, we apply binary geometries to trace close binarity among MYSOs. The inner sizes of MYSOs, Herbig AeBe and T Tauri stars appear to follow a universal trend at which the sizes scale with the square-root of the stellar luminosity. The Brgamma emission originates from somewhat smaller and co-planar area compared to the 2.2 μm continuum emission. We discuss this new finding with respect to disc-wind or jet origin. Finally, we report an MYSO binary fraction of 17-25% at milli-arcsecond separations (2-300 au). The size-luminosity diagram indicates that the inner regions of discs around young stars scale with luminosity independently of the stellar mass. At the targeted scales (2-300 au), the MYSO binary fraction is lower than what was previously reported for the more evolved main sequence massive stars, which, if further confirmed, could implicate the predictions from massive binary formation theories. Lastly, we spatially resolve the crucial star/disc interface in a sample of MYSOs, showing that au-scale discs are prominent in high-mass star formation and similar to their low-mass equivalents.

12. The IGRINS YSO Survey I. Stellar parameters of pre-main sequence stars in Taurus-Auriga

Ricardo López-Valdivia, Kimberly R. Sokal, Gregory N. Mace, Benjamin T. Kidder, Maryam Hussaini, Larissa Nofi, L. Prato, Christopher M. Johns-Krull, Heeyoung Oh, Jae-Joon Lee, Chan Park, Jae Sok Oh, Adam Kraus, Kyle F. Kaplan, Joe Llama, Andrew W. Mann, Hwihyun Kim, Michael A. Gully-Santiago, Hye-In Lee, Soojong Pak, Narae Hwang, Daniel T. Jaffe

We present fundamental parameters for 110 canonical K- & M-type ($1.3-0.13 M_{\odot}$) Taurus-Auriga young stellar objects (YSOs). The analysis produces a simultaneous determination of effective temperature ($T_{\rm eff}$), surface gravity (log g), magnetic field strength (B), and projected rotational velocity ($v \sin i$). Our method employed synthetic spectra and high-resolution (R$\sim$45,000) near-infrared spectra taken with the Immersion GRating INfrared Spectrometer (IGRINS) to fit specific K-band spectral regions most sensitive to those parameters. The use of these high-resolution spectra reduces the influence of distance uncertainties, reddening, and non-photospheric continuum emission on the parameter determinations. The median total (fit + systematic) uncertainties were 170 K, 0.28 dex, 0.60 kG, 2.5 km s^{-1} for $T_{\rm eff}$, log g, B, and $v \sin i$, respectively. We determined B for 41 Taurus YSOs (upper limits for the remainder) and find systematic offsets (lower $T_{\rm eff}$, higher log g and $v \sin i$) in parameters when B is measurable but not considered in the fit. The average log g for the Class II and Class III objects differs by 0.23$\pm$0.05dex, which is consistent with Class III objects being the more evolved members of the star-forming region. However, the dispersion in log g is greater than the uncertainties, which highlights how the YSO classification correlates with age (log g), yet there are exceptionally young (lower log g) Class III YSOs and relatively old (higher log g) Class II YSOs with unexplained evolutionary histories. The spectra from this work are provided in an online repository along with TW Hydrae Association (TWA) comparison objects and the model grid used in our analysis.

13. If you like C/O variations, you should have put a ring on it

Nienke van der Marel, Arthur Bosman, Sebastiaan Krijt, Gijs D. Mulders, Jennifer B. Bergner

The C/O-ratio as traced with C_2H emission in protoplanetary disks is fundamental for constraining the formation mechanisms of exoplanets and our understanding of volatile depletion in disks, but current C_2H observations show an apparent bimodal distribution which is not well understood, indicating that the C/O distribution is not described by a simple radial dependence. The transport of icy pebbles has been suggested to alter the local elemental abundances in protoplanetary disks, through settling, drift and trapping in pressure bumps resulting in a depletion of volatiles in the surface and an increase of the elemental C/O. We combine all disks with spatially resolved ALMA C_2H observations with high-resolution continuum images and constraints on the CO snowline to determine if the C_2H emission is indeed related to the location of the icy pebbles. We report a possible correlation between the presence of a significant CO-icy dust reservoir and high C_2H emission, which is only found in disks with dust rings outside the CO snowline. In contrast, compact dust disks (without pressure bumps) and warm transition disks (with their dust ring inside the CO snowline) are not detected in C_2H, suggesting that such disks may never have contained a significant CO ice reservoir. This correlation provides evidence for the regulation of the C/O profile by the complex interplay of CO snowline and pressure bump locations in the disk. These results demonstrate the importance of including dust transport in chemical disk models, for a proper interpretation of exoplanet atmospheric compositions, and a better understanding of volatile depletion in disks, in particular the use of CO isotopologues to determine gas surface densities.

14. The Mass Budgets and Spatial Scales of Exoplanet Systems and Protoplanetary Disks

Gijs D. Mulders, Ilaria Pascucci, Fred J. Ciesla, Rachel B. Fernandes

Planets are born from disks of gas and dust, and observations of protoplanetary disks are used to constrain the initial conditions of planet formation. However, dust mass measurements of Class II disks with ALMA have called into question whether they contain enough solids to build the exoplanets that have been detected to date. In this paper, we calculate the mass and spatial scale of solid material around Sun-like stars probed by transit and radial velocity exoplanet surveys, and compare those to the observed dust masses and sizes of Class II disks in the same stellar mass regime. We show that the apparent mass discrepancy disappears when accounting for observational selection and detection biases. We find a discrepancy only when the planet formation efficiency is below 100%, or if there is a population of undetected exoplanets that significantly contributes to the mass in solids. We identify a positive correlation between the masses of planetary systems and their respective orbital periods, which is consistent with the trend between the masses and the outer radii of Class II dust disks. This implies that, despite a factor 100 difference in spatial scale, the properties of protoplanetary disks seem to be imprinted on the exoplanet population.

15. The IMF and multiplicity of stars from gravity, turbulence, magnetic fields, radiation and outflow feedback

Sajay Sunny Mathew, Christoph Federrath

We perform a series of three-dimensional, magnetohydrodynamical (MHD) simulations of star cluster formation including gravity, turbulence, magnetic fields, stellar radiative heating and outflow feedback. We observe that the inclusion of protostellar outflows (1) reduces the star formation rate by a factor of ~ 2, (2) increases fragmentation, and (3) shifts the initial mass function (IMF) to lower masses by a factor of 2.0 ± 0.2, without significantly affecting the overall shape of the IMF. The form of the sink particle (protostellar objects) mass distribution obtained from our simulations matches the observational IMFs reasonably well. We also show that turbulence-based theoretical models of the IMF agree well with our simulation IMF in the high-mass and low-mass regime, but do not predict any brown dwarfs, whereas our simulations produce a considerable number of sub-stellar objects, which are produced by dynamical interactions (ejections). We find that these dynamical interactions also play a key role for the binary separation distribution and stellar kinematics in general. Our numerical model of star cluster formation also reproduces the observed mass dependence of multiplicity. Our multiplicity fraction estimates generally concur with the observational estimates for different spectral types. We further calculate the specific angular momentum of all the sink particles and find that the average value of $1.5 \times 10^{19}\,\mathrm{cm^2\,s^{-1}}$ is consistent with observational data. The specific angular momentum of our sink particles lies in the range typical of protostellar envelopes and binaries. We conclude that the IMF is controlled by a combination of gravity, turbulence, magnetic fields, radiation and outflow feedback.

16. Bridging the gap between protoplanetary and debris disks: separate evolution of millimeter and micrometer-sized dust

Arnaud Michel, Nienke van der Marel, Brenda Matthews

The connection between the nature of a protoplanetary disk and that of a debris disk is not well understood. Dust evolution, planet formation, and disk dissipation likely play a role in the processes involved. We aim to reconcile both manifestations of dusty circumstellar disks through a study of optically thin Class III disks and how they correlate to younger and older disks. In this work, we collect literature and ALMA archival millimeter fluxes for 85 disks (8%) of all Class III disks across nearby star-forming regions. We derive millimeter-dust masses $M_{\rm dust}$ and compare these with Class II and debris disk samples in the context of excess infrared luminosity, accretion rate, and age. The mean $M_{\rm dust}$ of Class III disks is $0.29 \pm 0.19\ M_\oplus$. We propose a new evolutionary scenario wherein radial drift is very efficient for non-structured disks during the Class II phase resulting in a rapid decrease of $M_{\rm dust}$. However, we find long infrared protoplanetary disk timescales of $\sim$8 Myr, which are consistent with overall slow disk evolution. In structured disks, the presence of dust traps allows for the formation of planetesimal belts at large radii, such as those observed in debris disks. We propose therefore that the planetesimal belts in debris disks are the result of dust traps in structured disks, whereas protoplanetary disks without dust traps decrease in dust mass through radial drift and are therefore undetectable as debris disks after the gas has dissipated. These results provide a hypothesis for a novel view of disk evolution.

17. Spatial Statistics in Star Forming Regions: Is Star Formation Driven By Column Density Alone?

Brendan Retter, Jennifer Hatchell, Tim Naylor

Star formation is known to occur more readily where more raw materials are available. This is often expressed by a 'Kennicutt-Schmidt' relation where the surface density of Young Stellar Objects (YSOs) is proportional to column density to some power, μ. The aim of this work was to determine if column density alone is sufficient to explain the locations of Class 0/I YSOs within Serpens South, Serpens Core, Ophiuchus, NGC1333 and IC348, or if there is clumping or avoidance that would point to additional influences on the star formation. Using the O-ring test as a summary statistic, 95 per cent confidence envelopes were produced for different values of μ from probability models made using the Herschel column density maps. The YSOs were tested against four distribution models: the best-estimate of μ for the region, $\mu = 0$ above a minimum column density threshold and zero probability elsewhere, $\mu = 1$, and the power-law that best represents the five regions as a collective, $\mu = 2.05 \pm 0.20$. Results showed that $\mu = 2.05$ model was consistent with the majority of regions and, for those regions, the spatial distribution of YSOs at a given column density is consistent with being random. Serpens South and NGC1333 rejected the $\mu = 2.05$ model on small scales of ~ 0.15pc which implies that small-scale interactions may be necessary to improve the model. On scales above 0.15 pc, the positions of YSOs in all five regions can be well described using column density alone.

18. An orbital release model for the Orion BN/KL fingers

A. C. Raga, P. R. Rivera-Ortiz, A. Rodriguez-Gonzalez, A. Castellanos-Ramirez

We present a simple model in which the bullets that produce the "Orion fingers" (ejected by the BN/KL object) are interpreted as protoplanets or low mass protostars in orbit around a high mass star that has a supernova explosion. As the remnant of the SN explosion has only a small fraction of the mass of the pre-supernova star, the orbiting objects then move away in free trajectories, preserving their orbital velocity at the time of release. We show that a system of objects arranged in approximately co-planar orbits results in trajectories with morphological and kinematical characteristics resembling the Orion fingers. We show that, under the assumption of constant velocity motions, the positions of the observed heads of the fingers can be used to reconstruct the properties of the orbital structure from which they originated, resulting in a compact disk with an outer radius of ~ 2.4 AU.

19. A Core Mass Function Indistinguishable from the Salpeter Stellar Initial Mass Function Using 1000 au Resolution ALMA Observations

Genaro Suárez, Roberto Galván-Madrid, Luis Aguilar, Adam Ginsburg, Sundar Srinivasan, Hauyu Baobab Liu, Carlos G. Román-Zúñiga

We present the core mass function (CMF) of the massive star-forming clump G33.92+0.11 using 1.3 mm observations obtained with the Atacama Large Millimeter/submillimeter Array (ALMA). With a resolution of 1000 au, this is one of the highest resolution CMF measurements to date. The CMF is corrected by flux and number incompleteness to obtain a sample that is complete for gas masses $M \gtrsim 2.0\ M_{\odot}$. The resulting CMF is well represented by a power-law function ($dN/d\log M \propto M^{\Gamma}$), whose slope is determined using two different approaches: *i*) by least-squares fitting of power-law functions to the flux- and number-corrected CMF, and *ii*) by comparing the observed CMF to simulated samples with similar incompleteness. We provide a prescription to quantify and correct a flattening bias affecting the slope fits in the first approach, which is caused by small-sample or edge effects when the data is represented by either classical histograms or a kernel density estimate, respectively. The resulting slopes from both approaches are in good agreement each other, with $\Gamma = -1.11^{+0.12}_{-0.11}$ being our adopted value. Although this slope appears to be slightly flatter than the Salpeter slope $\Gamma = -1.35$ for the stellar initial mass function (IMF), we find from Monte Carlo simulations that the CMF in G33.92+0.11 is statistically indistinguishable from the Salpeter representation of the stellar IMF. Our results are consistent with the idea that the form of the IMF is inherited from the CMF, at least at high masses and when the latter is observed at high-enough resolution.

20. Optical Properties of Interstellar Dust around the Orion A Molecular Cloud

Hayato Uehara, Kazuhito Dobashi, Shingo Nishiura, Tomomi Shimoikura, Takahiro Naoi

We have studied optical properties of interstellar dust around the Orion A molecular cloud to investigate the size distribution and the composition of dust grains. Orion A is one of the most studied molecular clouds in the solar vicinity ($d \simeq 400$ pc). In this paper, we used optical and near-infrared photometric data. The optical data were obtained by $BVRI$ bands imaging observations. The near-infrared data consisting of JHK_S bands were taken from 2MASS point source catalog. We produced some color excess maps around Orion A, and measured their ratios such as $E(R-I)/E(B-V)$. In order to investigate dust properties, we compared the observed ratios with results of simulation performed by Naoi T. et al. (2021) who calculated the extinction in the optical to near-infrared wavelengths based on a standard dust model; they assumed a power-law grain-size distribution with an upper cutoff radius and assumed *graphite* and *silicate* as dominant components. As a result, we found that the upper cutoff radius around Orion A is $\simeq 0.3\ \mu$m, and *silicate* predominates compared with *graphite* (with the fraction of *silicate* grater than 93 %). In addition, we further derived the total-to-selective extinction ratio R_V from the observed extinction of A_V and the color excess $E(B-V)$, and compared it with the model calculations. Dust properties (i.e., the upper cutoff radius and the ratio of *graphite*/*silicate*) derived from R_V is almost consistent with those derived from the color excess ratios.

21. Probing Protoplanetary Disk Winds with C II Absorption

Ziyan Xu, Gregory J. Herczeg, Christopher M. Johns-Krull, Kevin France

We present an analysis of wind absorption in the C II λ1335 doublet towards 40 classical T Tauri stars with archival far-ultraviolet (FUV) spectra obtained by the Hubble Space Telescope. Absorption features produced by fast or slow winds are commonly detected (36 out of 40 targets) in our sample. The wind velocity of the fast wind decreases with disk inclination, consistent with expectations for a collimated jet. Slow wind absorption is detected mostly in disks with intermediate or high inclination, without a significant dependence of wind velocity on disk inclination. Both the fast and slow wind absorption are

preferentially detected in FUV lines of neutral or singly ionized atoms. The Mg II $\lambda\lambda 2796, 2804$ lines show wind absorption consistent with the absorption in the C II lines. We develop simplified semi-analytical disk/wind models to interpret the observational disk wind absorption. Both fast and slow winds are consistent with expectations from a thermal-magnetized disk wind model and are generally inconsistent with a purely thermal wind. Both the models and the observational analysis indicate that wind absorption occurs preferentially from the inner disk, offering a wind diagnostic in complement to optical forbidden line emission that traces the wind in larger volumes.

22. TIMES II: Investigating the Relation Between Turbulence and Star-forming Environments in Molecular Clouds

Hyeong-Sik Yun, Jeong-Eun Lee, Neal J. Evans II, Stella S. R. Offner, Mark H. Heyer, Jungyeon Cho, Brandt A. L. Gaches, Yao-Lun Yang, How-Huan Chen, Yunhee Choi, Yong-Hee Lee, Giseon Baek, Minho Choi, Jongsoo Kim, Hyunwoo Kang, Seokho Lee, Ken'ichi Tatematsu

We investigate the effect of star formation on turbulence in the Orion A and Ophiuchus clouds using principal component analysis (PCA). We measure the properties of turbulence by applying PCA on the spectral maps in ^{13}CO, C^{18}O, HCO$^+$ J =1−0, and CS J =2−1. First, the scaling relations derived from PCA of the ^{13}CO maps show that the velocity difference (δv) for a given spatial scale (L) is the highest in the integral shaped filament (ISF) and L1688, where the most active star formation occurs in the two clouds. The δv increases with the number density and total bolometric luminosity of the protostars in the sub-regions. Second, in the ISF and L1688 regions, the δv of C^{18}O, HCO$^+$, and CS are generally higher than that of ^{13}CO, which implies that the dense gas is more turbulent than the diffuse gas in the star-forming regions; stars form in dense gas, and dynamical activities associated with star formation, such as jets and outflows, can provide energy into the surrounding gas to enhance turbulent motions.